

Heat- and mass-transport in aqueous silica nanofluids

A. N. Turanov · Yuriy V. Tolmachev

Received: 20 April 2009 / Accepted: 30 August 2009 / Published online: 16 September 2009
© Springer-Verlag 2009

Abstract Using the transient hot wire and pulsed field gradient nuclear magnetic resonance methods we determined the thermal conductivity and the solvent self-diffusion coefficient (SDC) in aqueous suspensions of quasi-monodisperse spherical silica nanoparticles. The thermal conductivity was found to increase at higher volume fraction of nanoparticles in accordance with the effective medium theory albeit with a smaller slope. On the other hand, the SDC was found to decrease with nanoparticle volume fraction faster than predicted by the effective medium theory. These deviations can be explained by the presence of an interfacial heat-transfer resistance and water retention by the nanoparticles, respectively. We found no evidence for anomalous enhancement in the transport properties of nanofluids reported earlier by other groups.

1 Introduction

Anomalous transport properties of nanofluids (suspensions of nanoparticles in liquids) have become a subject of intense research recently [1–4]. Most efforts have been focused on so-called anomalous heat transfer enhancement, which means an increase in thermal conductivity beyond the predictions of the classical effective medium theory [5]. Other transport properties, such as tracer diffusion coefficient [6], have also been reported as anomalously high, and a connection between the heat- and mass-transport

enhancement has been proposed in microconvection-based theories [1, 7–9]. A large body of literature also reports that addition of nanoparticles to liquids can cause interfacial mass-transport rates, such as the rate of gas sorption into liquid under convection [10–14], to increase several times. As this phenomenon is more complex than transport in the bulk of stagnant liquid, and may involve contributions from interfacial area, hydrodynamic boundary layer thickness, adsorption of the gas on the nanoparticles, etc., it seems appropriate to investigate first the intrinsic mass-transport in nanofluids in absence of convective, interfacial and other complicating effects.

The goals of the present study were to determine the thermal conductivity and the solvent self-diffusion coefficient (SDC) of silica nanofluids studied previously in the context of thermal conductivity enhancement [15, 16]. The thermal conductivity was measured using the transient hot wire method employed in our earlier work on alumina nanofluids [4]. For the measurement of the proton SDC, we used pulsed field gradient nuclear magnetic resonance (PFG NMR) method. This is a well-established technique for diffusion studies in liquids in the time scale from a few milliseconds to a few seconds [17, 18], and it has been applied successfully to study both the solvent self-diffusion [19–21] as well as the nanoparticle diffusion [22–24] in colloidal suspensions.

2 Experimental

The samples used in our study were Ludox brand aqueous suspension of colloidal silica (Grace Davison). According to the manufacturer and previous studies [16], they contain quasi-monodisperse non-agglomerated spherical nanoparticles suspended in a dilute (mM) aqueous carbonate buffer

A. N. Turanov · Y. V. Tolmachev (✉)
Department of Chemistry, Kent State University,
Kent, OH 44240, USA
e-mail: ytolmach@kent.edu

A. N. Turanov
Zavoisky Physical-Technical Institute, 420029 Kazan, Russia

at pH 9. Additional data on the structure of the nanofluids are provided in our forthcoming publication [25]. The properties of the stock solutions are summarized in Table 1. We would like to note here that we calculated the volume fraction of nanoparticles on the basis of the experimentally determined mass fraction of nanoparticles and density of nanofluid rather than using assumptions about the density of nanoparticles. Although the nanoparticle densities calculated this way are noticeably higher (2.51 g/cm³ in for SM, 2.36 for HM and TM, and 2.33 for INPBE) than those assumed in earlier studies (2.2 g/cm³ in Ref. [16]), the resulting differences in volume fractions are insignificant ($\leq 1\%$). The stock solutions were diluted, if needed, using ultrapure water produced with Nanopure Diamond apparatus (Barnstead) with the resistivity $>18.2 \text{ M } \Omega \text{ cm}^{-1}$ and <2 ppb of total organic carbon.

For the thermal conductivity measurements we used a transient-hot wire thermal property analyzer (KD2pro from Decagon Devices Inc.). The details of our experimental set up can be found in Ref. [4] The values we obtained for thermal conductivity of pure water [$0.608 \pm 0.002 \text{ W/(m K)}$] at $20 \pm 0.5^\circ\text{C}$ are slightly higher than the reference value [$0.597 \pm 0.001 \text{ W/(m K)}$] [26]. Based on our extensive earlier studies we attribute this discrepancy to a convective effect in water. Such effects are expected to be smaller in nanofluids which have higher viscosities. At any rate, the magnitude of the discrepancy even in water is within 1.5% and it is smaller than the effects on which this work is focused.

The NMR measurements have been performed at $20 \pm 0.5^\circ\text{C}$ (unless stated otherwise) on water protons using Varian Unity/Inova 500 MHz spectrometer equipped with narrow-bore Varian XYZ gradient probe with a maximum gradient strength 28 G/cm in X or Y direction. To minimize convection in the liquid samples, 1.6 mm inner diameter NMR tubes were used. The height of the liquid samples was 15 mm which is within the region of a uniform magnetic field gradient of the probe.

The SDC was measured by means of Stejskal–Tanner sequence ($90^\circ\text{--}\tau\text{--}180^\circ\text{--}\tau$ echo) with PFGs [27]. The main magnetic field was in the Z direction (vertically). Pulsed gradients of duration $\delta = 2 \text{ ms}$ were applied perpendicular to the main magnetic field after $\tau = 50 \text{ ms}$ the first 90° (4.1 μs) and second 180° (8.2 μs) pulses. Thus, the peaks of the gradient pulses are separated by the diffusion time $\Delta = 100 \text{ ms}$. The gradients, G , were varied in five to ten steps up to the gradient of 17.5 G/cm. We did not use the maximum gradient to avoid the occurrence of temperature gradients and a mechanical “ringing” of coils. A delay of 10 s was applied before every pulse sequence to allow for a full equilibration of the protons polarization (in our samples $T_1 = T_2 \in [0.5 \text{ s}; 2.0 \text{ s}]$). In the experiments dealing with the time dependence of the diffusion coefficient, Δ was varied between 10 and 750 ms.

The NMR signal, A , was obtained by integrating the Fourier transform of the echo signal. Signal attenuation due to unrestricted random walk diffusion is given by the Stejskal–Tanner formula [27]

$$\ln\left(\frac{A}{A_0}\right) = -\gamma^2 G^2 D \delta^2 \left(\Delta - \frac{\delta}{3}\right), \quad (1)$$

where D and γ are the SDC and the gyromagnetic ratio of the protons, A_0 is A at $G = 0$. In order to obtain an adequate signal to noise ratio in the measurements of D , we averaged A values of 16 scans cycling the phases of 90° and 180° pulses. A versus G data were repeated for each sample at least five times on different days and the standard deviations of D shown in this work reflect this repeatability. Additional experiments, where G was varied keeping $G\delta$ constant, proved the heating of the gradient coils was not the limiting factor in the precision of these measurements. In our opinion, the precision (and accuracy) of D is determined by the long-term stability of the temperature control, which in turn influences the convection in the samples. All error bars and uncertainties for experimental values in this paper refer to the standard deviation

Table 1 Properties of Ludox brand colloidal silica suspensions

Name	Mass fraction (%) ^a	Nanofluid density (g/cm ³) ^a	Volume fraction (%) ^b	Particle diameter (nm) (from surface area) ^a	Particle diameter (nm)
Ludox SM	30.0	1.22	14.6	8.4	10.7 ± 4.9^c
Ludox HM	40.0	1.30	22	12.9	16.7 ± 4.3^c
Ludox TM	40.0	1.30	22	23	28.6 ± 6.8^c
Ludox INPBE	50.0	1.40	30	22	20–30 ^d

^a Reported by the manufacturer

^b Calculated using mass fraction of nanoparticles and density of nanofluid

^c From small angle X-ray scattering data in Ref. [16]

^d From TEM and DLS data in Ref. [25]

estimated from a series of consecutive measurements rather than to a standard error of the mean.

3 Results and discussion

3.1 Thermal conductivity of nanofluids

Figure 1 displays the results of our thermal conductivity measurement of different colloidal silica suspensions. The dependence of normalized thermal conductivity k_{nf}/k_0 , where k_{nf} and k_0 are the thermal conductivity of the base fluid (water) and of the nanofluid, respectively, on the volume fraction of colloidal particles, ϕ , is given in the effective medium theory by Eq. 2 [1, 4]:

$$\frac{k_{nf}}{k_0} = 1 + 3 \frac{k_1/k_0 - 1}{k_1/k_0 + 2} \phi. \quad (2)$$

In the latter formula, k_1 is the thermal conductivity of the material of the colloidal particles, and this equation is strictly applicable only to spherical particles. The slope for the dependence shown in Fig. 1 predicted on the basis on Eq. 3 is 0.92 if the values of $k_0 = 0.605$ and $k_1 = 1.4$ W/(m K) are used as in Ref. [16]. The experimental results show a smaller slope, i.e. 0.53 ± 0.02 . The most likely reason for the thermal conductivity enhancement being below the prediction of Eq. 2 is the presence of Kapitza (heat-transfer) resistance on the interface between silica particles and water, as was noticed in our earlier paper dealing with alumina nanofluids [4]. In this case, the appropriate formula is [1, 4]

$$\frac{k_{nf}}{k_0} = 1 + 3 \frac{k_1/k_0 - 1}{k_1/k_0 + 2 + 2k_1/(R\beta)} \phi, \quad (3)$$

where R is the radius on the suspended particles and β is the interfacial thermal conductance. The introduction of the Kapitza resistance into consideration may explain the increase in the normalized conductivity with increase in the silica particle size reported in Ref. [16]. We believe that data in Fig. 1 are not sufficiently accurate to draw reliable conclusions on the particle size effect. Instead, we estimate the upper and lower limits of β assuming 5 and 15 nm particle radii, respectively. Such analysis leads to $\beta = (0.7\text{--}2.2) \times 10^8$ K/W, which has the same order of magnitude as the value we found earlier for the alumina/water interface (5×10^8 K/W) [4].

3.2 Solvent self-diffusion coefficient in nanofluids

Pulsed field gradient nuclear magnetic resonance diffusion measurements with pure water at $20 \pm 0.5^\circ\text{C}$ yielded the values for SDC of ^1H as $2.00 \pm 0.08 \times 10^{-9} \text{ m}^2 \text{ s}^{-1}$ which is close to the literature values obtained with the same technique, i.e. $2.025 \times 10^{-9} \text{ m}^2 \text{ s}^{-1}$ [28]. In following studies we focused on ^1H SDC measurements with Ludox TM samples at different dilutions.

For all studied samples and diffusion times the dependence of the echo amplitude, A , on the square of the magnetic field gradient, G^2 , followed a single exponential decay predicted by (1) in the whole range of the gradients studied (1.5 decades in A , see Fig. 2). No time dependence of D was observed for any of the samples in the range of

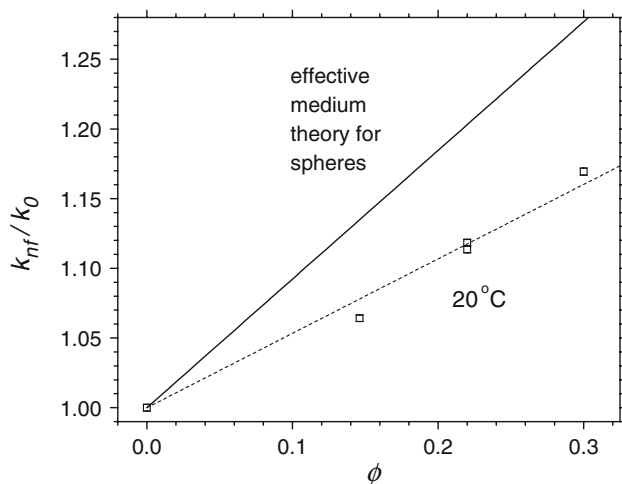


Fig. 1 Normalized thermal conductivity of different colloidal silica suspensions at 20°C plotted versus the volume fraction of the nanoparticles (squares). The dashed line is the best linear fit with a fixed intercept of 1. The solid line is calculated based on Eq. 2. The standard deviation in k_{nf}/k_0 is approximately the same as the height of the symbols used

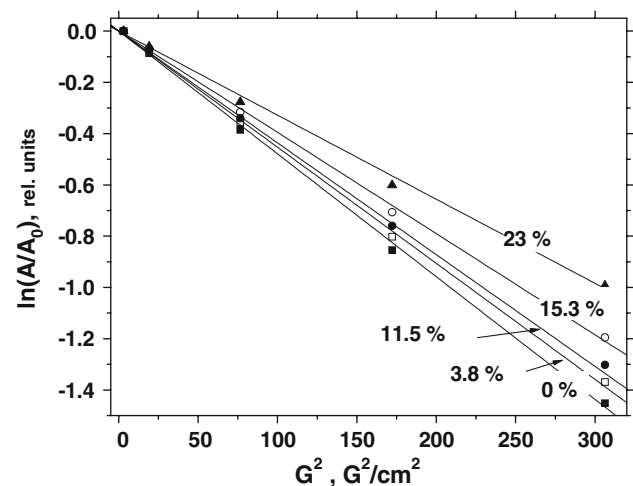


Fig. 2 Stejskal–Tanner plots for Ludox TM colloidal silica at different volume fraction of the nanoparticles (filled squares 0%, open squares 3.8%, filled circles 11.5%, open circles 15.3%, filled triangles 23%). The standard deviation in $\ln(A/A_0)$ is smaller than the height of the symbols used

10 ms $\leq \Delta \leq$ 750 ms (see Fig. 3) within the precision of our experiment (relative standard deviation of 4%).

At short times Δ , normal diffusion, with the solvent SDC value the same as for pure solvent, can be expected. At longer times, when the distance that the solvent molecules travel within the duration of the experiment, Δ , becomes comparable to the distance between the obstructive particles, d , a third regime, restricted diffusion, with the solvent SDC decreasing with time, is expected to show up. For particles with $R = 10$ nm, the values of d are 18 and 66 nm for $\phi = 0.22$ and $\phi = 0.04$, respectively, if the hexagonal close packing is assumed for calculating d , i.e. $d = \left\{ \sqrt[3]{\frac{8\pi}{3\sqrt{3}\phi}} - 2 \right\} R$. Therefore, the transition to restricted diffusion regime should start around $\Delta_{RD} = 27$ ns for $\phi = 0.22$ and 363 ns for $\phi = 0.04$, respectively. Finally, at even longer times Δ , when the solvent molecules travel distances significantly larger than the distance between the suspended nanoparticles, the volume-averaged solvent SDC reaches a constant lower value determined by the excluded volume of the obstructive phase [29]. Since PFG NMR diffusivity measurements are limited at present to the experiments with Δ orders of magnitude larger than Δ_{RD} calculated above, we expect to work in the excluded volume diffusion regime. It should be noted here that the mean square displacement of the solvent molecule changes linearly with time only under the normal and excluded volume diffusion regimes, and that under the intermediate restricted diffusion regime Eq. 1 is not valid.

Under the excluded volume diffusion regime, one can expect a reduction in the value of D with the increase of the

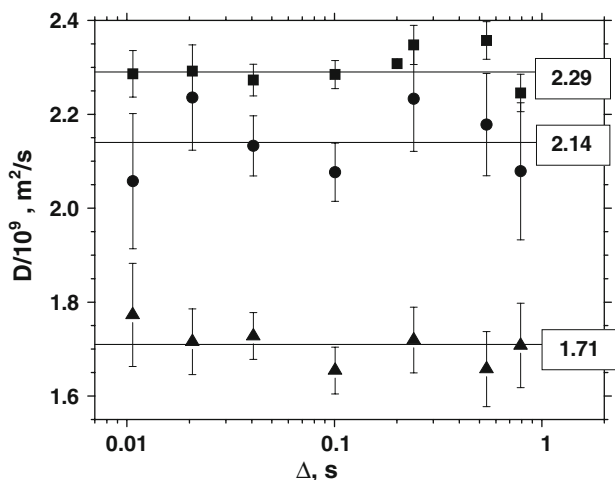


Fig. 3 Time dependence of the ^1H SDC of selected samples (filled squares $\phi = 0\%$, filled circles $\phi = 11.5\%$, filled triangles $\phi = 23\%$) as determined by PFG NMR. These data were obtained at 25°C and they show a bigger scatter than we observed at 20°C in other experiments because of the convection induced by temperature control. The solid lines and the numbers in boxes show the average value of D for given ϕ

volume fraction of the obstructive phase (nanoparticles), i.e. the behavior we found experimentally (see Fig. 4). The simplest theory (spherical particles in spherical cells) gives the following result for the obstruction (excluded volume) effect [29]:

$$\frac{D}{D_0} = \frac{1}{1 + 0.5\phi} \quad (4)$$

where D_0 is the solvent SDC in pure solvent, D is the macroscopic (volume averaged) solvent SDC in the suspension, and ϕ is the volume fraction of the particles. Corrections to this formula within a lattice model have been developed in Ref. [20] but they are important only for $\phi > 0.5$ and can be neglected here. The data in Fig. 4 show that the reduction of the D upon increase in ϕ is larger than predicted by Eq. 4. Particularly interesting is the fact that (4) predicts the limit of $D/D_0 = 2/3$ at $\phi = 1$, but experimentally this value of D/D_0 is reached at $\phi = 0.25$. Thus, we turned our attention to other factors which may contribute to a larger-than-expected decrease of the macroscopic solvent SDC in the nanofluids.

Because Ludox TM colloids are known to consist of fairly monodisperse spherical particles and because the shape of D versus ϕ for spheroidal particles is predicted to be convex [29] rather than concave as found in this work (Fig. 4) we did not consider the particle shape effects. This exclusion is further validated by the fact that if a fitting using Eq. (1.3) from Ref. [20] is attempted, an unreasonable value of the form factor (0.75) is obtained. Also, the polydispersity and disorder of the position of nanoparticles is expected to increase rather than decrease D [29].

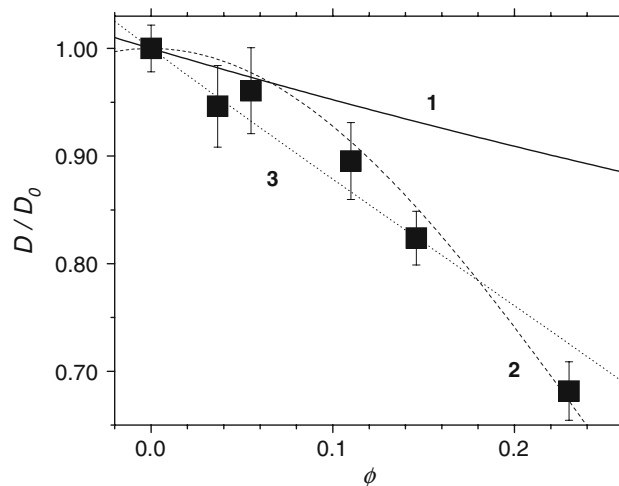


Fig. 4 Dependence of the ^1H SDC (normalized to SDC in pure water, D_0) in Ludox TM nanofluids on the volume fraction of nanoparticles (filled squares) and the best fits from different models (see text): line 1 (solid) $Y = 1/(1 + 0.5X)$; line 2 (dash) $Y = \exp\{-7.5X^2\}$; line 3 (dot) $Y = (1 - 1.5X)/\{(1 - X)(1 + 0.5 \times 1.5X)\}$

On the other hand, silica is well known for its hygroscopic properties; therefore, the adsorption of water onto (and even absorption into) the nanoparticles resulting in the partition of the solvent between fast “free” water and slow “bound” fractions should be considered.

The obstructive effects of dissolved polymers on solvent SDC have been modeled using (5) [30]. This model also worked well for other colloidal suspensions with solvent penetrating the particles [21]. This formula gives a better fit to our data (with $\alpha = 7.5$ and $\nu = 2$) but the physical meaning of the adjustable parameters remains elusive [21].

$$\frac{D}{D_0} = \exp(-\alpha\phi^\nu) \quad (5)$$

A better fit can also be obtained using Eq. 6 derived under assumption of solvent layering around the particle [19]:

$$\frac{D}{D_0} = \frac{1 - k^3\phi}{(1 - \phi)(1 + 0.5k^3\phi)}, \quad (6)$$

where k is the ratio of hydrodynamic particle radius to the radius of the solid particle core. In our case, the fitting gives $k = 1.5^{1/3} = 1.145$. This corresponds to a water layer of 1.67 nm, or six water molecules (assuming 0.275 nm as water molecule radius) [31]. Other formulas derived for layering type of corrections (Eqs. 28 and 32 in Ref. [29]) did not produce a better fit or required unphysical values of adjustable parameters.

Our observation of the reduction of the solvent diffusion coefficient with the increase in the nanoparticle volume fraction, and, more specifically, a reduction larger than predicted by the simple excluded volume model, agrees with recent data obtained with aqueous suspension of alumina particles of somewhat larger size (50 nm) [32].

4 Conclusion

We measured thermal conductivity and solvent SDC in well-characterized quasi-monodisperse suspensions of silica nanoparticles in water. We did not find anomalous enhancement in either property. In fact, the observed values of the thermal conductivities and solvent SDC as a function of the volume fraction of nanoparticles are below the predictions of the simple effective medium theory; and the deviations can be explained by interaction of the water with the silica particles. The results of our combined heat- and mass-transport study agree with recent experimental [4, 32, 33] and theoretical [4, 34] findings that disprove the existence of anomalous enhancement in the transport properties of nanofluids.

Acknowledgments We thank Prof. A. Khitrin for his invaluable assistance with NMR experiments and critical comments regarding

the manuscript, as well as Prof. S. Sprunt, Prof. B. Ellman and Prof. J. Selinger for productive discussions and their support during the project. Our acknowledgements also go to the participants of International Nanofluid Property Benchmark Exercise, especially its organizer Prof. Jacopo Buongiorno, for providing us with a Ludox INPBE sample and with Ref. [32]. This research was supported by the US Office of Naval Research and by the Ohio Board of Regents.

References

1. Das SK, Choi SUS, Yu W, Pradeep T (2008) Nanofluids: science and technology. Wiley, Hoboken
2. Kabelac S, Kuhnke JF (2006) Heat transfer mechanisms in nanofluids—experiments and theory. Ann Assembly Int Heat Transf Conf 13:KN-11
3. Gandhi KS (2007) Thermal properties of nanofluids: controversy in the making? Curr Sci 92:717–718
4. Timofeeva EV, Gavrilov AN, McCloskey JM, Tolmachev YV, Sprunt S, Lopatina LM, Selinger JV (2007) Thermal conductivity and particle agglomeration in alumina nanofluids: experiment and theory. Phys Rev E Stat Nonlinear Soft Matter Phys 76:061203
5. Das SK, Choi SUS, Patel HE (2006) Heat transfer in nanofluids—a review. Heat Transf Eng 27:3–19
6. Krishnamurthy S, Bhattacharya P, Phelan PE, Prasher RS (2006) Enhanced mass transport in nanofluids. Nano Lett 6:419–423
7. Kumar DH, Patel HE, Kumar VRR, Sundararajan T, Pradeep T, Das SK (2004) Model for heat conduction in nanofluids. Phys Rev Lett 93:144301
8. Prasher R, Bhattacharya P, Phelan PE (2005) Thermal conductivity of nanoscale colloidal solutions (nanofluids). Phys Rev Lett 94:025901/1–025901/4
9. Patel HE, Sundararajan T, Pradeep T, Dasgupta A, Dasgupta N, Das SK (2005) A micro-convection model for thermal conductivity of nanofluids. Pramana J Phys 65:863–869
10. Olle B, Bucak S, Holmes TC, Bromberg L, Hatton TA, Wang DIC (2006) Enhancement of oxygen mass transfer using functionalized magnetic nanoparticles. Ind Eng Chem Res 45:4355–4363
11. Nagy E, Feczko T, Koroknai B (2007) Enhancement of oxygen mass transfer rate in the presence of nanosized particles. Chem Eng Sci 62:7391–7398
12. Komati S, Suresh AK (2008) CO₂ absorption into amine solutions: a novel strategy for intensification based on the addition of ferrofluids. J Chem Technol Biotechnol 83:1094–1100
13. Zhu HY, Shanks BH, Heindel TJ (2008) Enhancing CO-water mass transfer by functionalized MCM41 nanoparticles. Ind Eng Chem Res 47:7881–7887
14. Kang YT, Kim HJ, Lee KI (2008) Heat and mass transfer enhancement of binary nanofluids for H₂O/LiBr falling film absorption process. Int J Refrig 31:850–856
15. Milanova D, Kumar R (2005) Role of ions in pool boiling heat transfer of pure and silica nanofluids. Appl Phys Lett 87:233207 1–3
16. Chen G, Yu W, Singh D, Cookson D, Routbort J (2008) Application of SAXS to the study of particle-size-dependent thermal conductivity in silica nanofluids. J Nanopart Res 10:1109–1114
17. Stejskal EO (1971) Spin-echo measurement of self-diffusion in colloidal systems. Adv Mol Relax Prop 3:27–42
18. Weingaertner H, Holz M (2002) NMR studies of self-diffusion in liquids. Annu Rep Prog Chem Sect C 98:121–155
19. Von Meerwall E, Mahoney D, Iannacchione G, Skowronski D (1990) Concentration-dependence of solvent diffusion in a colloidal suspension. J Colloid Interf Sci 139:437–445
20. Venema P, Struis RPWJ, Leyte JC, Bedeaux D (1991) The effective self-diffusion coefficient of solvent molecules in colloidal crystals. J Colloid Interf Sci 141:360–373

21. Griffiths PC, Cheung AYP, Davies JA, Paul A, Tipples CN, Winnington AL (2002) Probing interactions within complex colloidal systems using PGSE-NMR. *Magn Reson Chem* 40:S40–S50
22. Wagner J, Hartl W, Walderhaug H (2001) Long time self-diffusion in suspensions of highly charged colloids: a comparison between pulsed field gradient NMR and Brownian dynamics. *J Chem Phys* 114:975–983
23. Valentini M, Vaccaro A, Rehor A, Napoli A, Hubbell JA, Tirelli N (2004) Diffusion NMR spectroscopy for the characterization of the size and interactions of colloidal matter: the case of vesicles and nanoparticles. *J Am Chem Soc* 126:2142–2147
24. Palit S, Yethiraj A (2008) A new model system for diffusion NMR studies of concentrated monodisperse and bidisperse colloids. *Langmuir* 24:3747–3751
25. Buongiorno J, Venerus D, Prabhat N (2009) A benchmark study on the thermal conductivity of nanofluids. *J Appl Phys* (submitted)
26. Vargaftik NB, Filipov LP, Tarzimanov AA, Totskii EE (1994) *Handbook of thermal conductivity of liquids and gases*. CRC Press, Boca Raton
27. Stejskal EO, Tanner JE (1965) Spin diffusion measurements: spin echoes in the presence of a time-dependent field gradient. *J Chem Phys* 42:288–292
28. Holz M, Heil SR, Sacco A (2000) Temperature-dependent self-diffusion coefficients of water and six selected molecular liquids for calibration in accurate ^1H NMR PFG measurements. *Phys Chem Chem Phys* 2:4740–4742
29. Joansson B, Wennerstroem H, Nilsson PG, Linse P (1986) Self-diffusion of small molecules in colloidal systems. *Colloid Polym Sci* 264:77–88
30. Phillies GDJ (1989) The hydrodynamic scaling model for polymer self-diffusion. *J Phys Chem* 93:5029–5039
31. Leng Y, Cummings PT (2006) Hydration structure of water confined between mica surfaces. *J Chem Phys* 124:074711/1–074711/4
32. Gerardi C, Cory D, Buongiorno J, Hu LW (2007) Nuclear magnetic resonance measurement of diffusion coefficients in alumina nanofluids. *Trans Am Nucl Soc* 96:485–486
33. Eapen J, Williams WC, Buongiorno J, Hu LW, Yip S, Rusconi R, Piazza R (2007) Mean-field versus microconvection effects in nanofluid thermal conduction. *Phys Rev Lett* 99:095901
34. Evans W, Fish J, Keblinski P (2006) Role of Brownian motion hydrodynamics on nanofluid thermal conductivity. *Appl Phys Lett* 88:093116 1–3